Trains of Taylor Bubbles over Hot Nano-Textured Mini-Channel Surface

Martin Freystein[1], Felix Kolberg[1], Lucas Spiegel[1], Sumit Sinha-Ray[2], Rakesh P. Sahu[2], Alexander L. Yarin[2,3*], Tatiana Gambaryan-Roisman[1*], Peter Stephan[1]

[1]*Institute of Technical Thermodynamics and Center of Smart Interfaces, Technische Universität Darmstadt, Alarich-Weiss-Str. 10, 64287 Darmstadt, Germany*

[2]*Department of Mechanical and Industrial Engineering, University of Illinois at Chicago, Chicago, Illinois 60607, USA*

[3]*College of Engineering, Korea University, Seoul 136-713, Republic of Korea*

Abstract

To enhance heat transfer in forced convective boiling the microchannel bottom was amended by nano-textured structures - periodic rectangular mats of electrospun polymer nanofibers. The fibers were about several hundreds of nanometer in cross-section. The test fluid was FC-72 and the flow in microchannels contained trains of the Taylor bubbles. The role of the nanofibers was to retain the warm microchannel bottom wetted, to prevent dry-out and thus to enhance the heat removal rate. In the present experiments the time-average heat flux at the nanofiber-coated domains was found to be 1.6 times higher than that at the uncoated ones. Accordingly, a significant decrease (by 5-8 K) in the superheat was observed. The heat transfer coefficient at the nanofiber mat-coated domains was found to be an order of magnitude higher than that at the uncoated domains. Such significant enhancement of heat transfer results from the fact that nanofiber mats facilitate wetting of the surface under the passing Taylor bubbles, thus delaying formation of vapor layer at the channel bottom.

Keywords: Flow boiling, Electrospinning, Nanofibers, Taylor bubbles, Nano-textured surfaces.

1. Introduction

The need for removal of large amounts of heat from small-scale semiconductor units imposes extremely challenging requirements on cooling systems [1]. Flow boiling in micro- and mini-channels holds great potential for thermal management of high-power density miniature electronic devices. One of the most important flow regimes during flow boiling in micro- and mini-channels is the slug flow regime. In this regime large elongated vapor Taylor bubbles, with the smallest dimension restricted by the channel cross-section, flow in train along the channel. The heat transfer in this regime is determined by evaporation of thin film separating the elongated bubbles from the heated walls [2, 3]. However, the liquid film around the elongated bubbles has been shown to dry out partially or completely [3, 4], which adversely affects the heat transfer. One of the major problems in the enhancement of heat transfer during flow boiling in micro- and mini-channels is finding the way to keep the heater wall around the flowing elongated bubbles wetted.

Several previous attempts have been made to enhance heat transfer during nucleate boiling and flow boiling by modification of the heater surface [5-7]. In particular, nanowires have been fabricated at the walls of micro-channels using a two-step electroless etching process, which resulted in stabilization of flow and boiling process and increase of removed heat flux in certain cases by about 40% [6]. Nano-texturing have been also rendered by electrospun nanofibers to enhance heat removal rate from high-power microelectronics by drop/spray cooling and in pool boiling and to prevent Leidenfrost effect when coolant droplets impact onto high-temperature surfaces [8-16]. These results show that heat removal at such nano-textured surfaces can be as high as 1 kW/cm^2.

In the present work we demonstrate that using nano-textured mini-channel surfaces can prevent dry-out underneath the passing trains of the Taylor bubbles, which opens an effective way for heat transfer enhancement in forced convective boiling. This is achieved by amending the mini-channel bottom with nano-textured periodic rectangular mats of electrospun polymer nanofibers of ~100 nm in diameter. In the present mini-channel experiments the flow of fluorinert fluid FC-72 with trains of the Taylor bubbles over the nanofibers retained the heated channel bottom wetted. As a result, dry-out was prevented leading to an enhancement in heat removal rate. The time-average heat flux at the nanofiber-coated domains was found to be up to 1.6 times higher than that at the uncoated ones. Accordingly, a significant decrease (by 5-8 K) in the superheat was observed for the Reynolds numbers in the 313-432 range with the applied heat flux being in the 28-36 kW/m^2 range. An order of magnitude increase in the heat transfer coefficient has been revealed. The significant enhancement of the heat transfer results from the fact that nanofiber mats facilitate wetting of the surface under the passing Taylor bubbles, thus delaying formation of vapor layer at the channel bottom. The interstices of the nanofiber coating act as the nucleation sites facilitating formation of tiny bubbles, which eventually results in a higher heat removal rate from the surface at a reduced superheat.

2. Experimental method

2.1.Preparation of nanofiber mats

Polyacrylonitrile (PAN; M_w=150 kDa) was obtained from Polymer Inc., n-dimethyl formamide (DMF) anhydrous-99.8%, was obtained from Sigma-Aldrich. Electrospinning was conducted with the 9 wt% PAN solutions in DMF. A standard electrospinning setup [17-19] was used to prepare PAN nanofiber mats over the stainless steel foils (20-mm foils of X5CrNi18-10 steel). The nanofibers were electrospun on the foil for 45 s. The fiber diameter was in the 100-300 nm range and the mat thickness was in the 6-15 µm range. Various periodic nanofiber patch patterns of different size and pitch were obtained by removing sections of the original continuous nanofiber mats using ethanol-wetted cottons, without disturbing the corresponding nanofiber patch area and avoidng any scratch or serration on the foil and between the patches. The nanofiber mat adhesion to the foil was enhanced by the wetting the edges of the patches with ethanol while removing the extra material, which also helped to avoid any additional edge effect during the experiments.

2.2. Experimental setup and method for heat flux measurement

The experimental setup for investigation of flow boiling in a mini-channel, the instrumentation used, the experimental procedure and the data processing have been described in [4, 20]. The flow patterns and heat transfer during flow boiling of fluorinert fluid FC-72 have been studied in a rectangular mini-channel with a length of 80 mm and a cross-section of 2 mm $\times$ 0.5 mm. The cross-section of the channel is schematically shown in Fig. 1a. A stainless steel foil which was heated by the electrical current constituted the upper wall of the mini-channel. The foil was coated periodically over parts of the channel length by a nanofiber mat (Fig. 1b). The flow patterns were observed by a high-speed video camera (Photron FASTCAM 1024) through an acrylic glass window from below. The time-dependent temperature distribution at the backside of the heater foil was registered using the middle wave high-speed infrared camera Thermosensorik CMT 256 HMS from above. This camera with a sensor of 256×256 pixel^2 has been used to record the temperature distribution with a frame rate of 1000 Hz. A spatial resolution of the infrared camera of 29.27 μm/pixel has been used in the experiments illustrated in Fig. 5. All other data in this work have been collected at a spatial resolution of 50.89 μm/pixel. An in-situ temperature calibration procedure has been adopted. For determination of the instantaneous distribution of heat flux transferred to the fluid, the transient energy balance has been evaluated for every pixel within the foil based on the measured temperature field and taking into account the electrical resistance heating and the two-dimensional heat conduction within the foil. In the experiments the heat flux applied at the heater, q_h, and the flow Reynolds number, *Re*, have been varied.

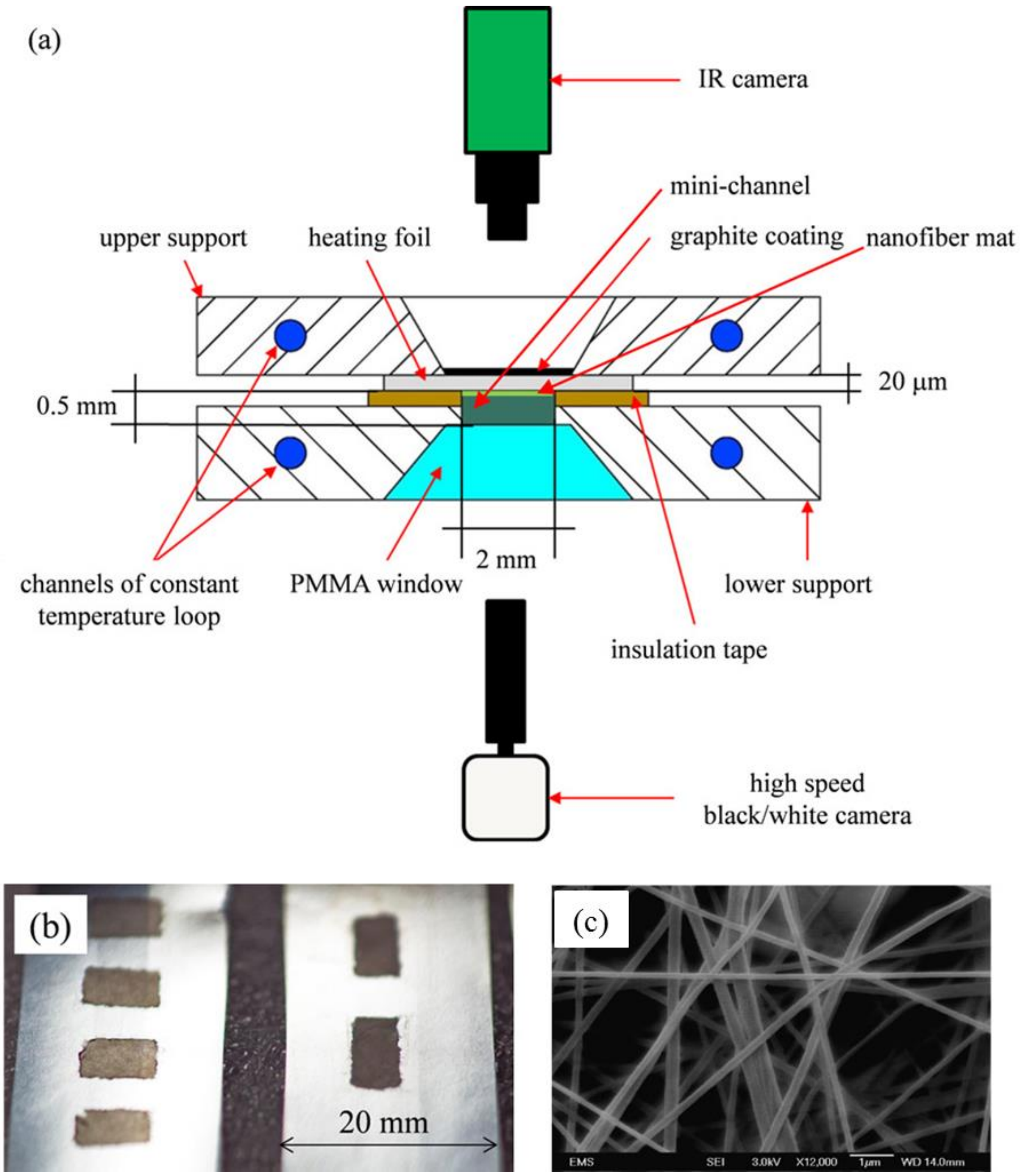

Fig. 1. (a) Schematic of experimental setup. (b) Periodic nano-textured sections on the mini-channel bottom. (c) A representative SEM image of nanofibers.

3. Results

In the first set of experiments the heater was covered by a continous nanofiber mat over a single region with a length exceeding 10 mm. A flow pattern near the boundary between the coated and uncoated regions, as well as the instantaneous distribution of heat flux, is shown in Fig. 2. The flow direction here and hereinafter is from right to left. A group of small bubbles seen in Fig. 2 in the image of the flow pattern is emerging at the boundary between the coated to uncoated parts of the heater. The bubbles move along the main flow direction and grow in time. In the same image a large advancing elongated Taylor bubble (or a slug) can be observed in the upstream part of the mini-channel. The observation of the instantaneous distribution of the heat flux reveals that the passage of bubbles over the uncoated part is accompanied by a strong local increase of heat flux in the vicinity of the moving contact line. This behavior agrees with the results of the earlier experiments [20] and with the model predictions [21]. The coated part of the heater is characterized by an approximately homogenous heat flux over a region with the length Δx=2.39 mm to the right of the boundary between the uncoated and coated part. This region is referred to as the transition region. The length of the transition region is a strongly decreasing function of the applied heat flux. For Re = 536 and q_h = 21.7 kW/m^2 this length is Δx=2.75 mm, whereas for Re = 536 and q_h = 29.8 kW/m^2 this length is reduced to Δx=1.02 mm. To the right of the transition region the heat flux transferred to the fluid is very low over a large area of the heater.

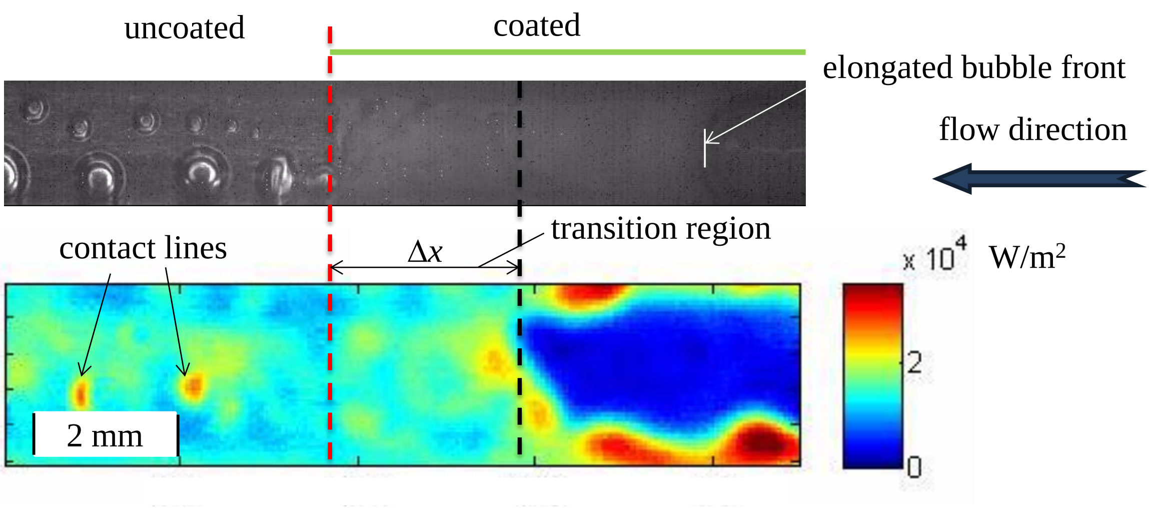

Fig. 2. Flow pattern and instantaneous heat flux distribution in a mini-channel with a single continuous nanofiber-coated patch. Re = 774, q_h = 21.9 kW/m^2.

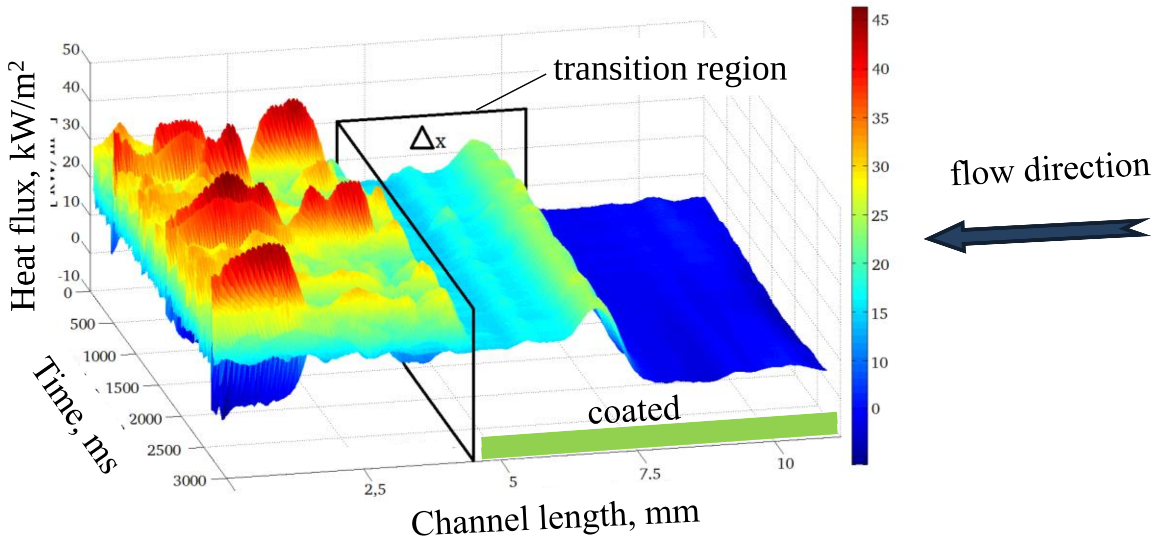

Fig. 3. Temporal evolution of the heat flux distribution in a mini-channel with a single nanofiber-coated patch. *Re* = 774, q_h = 21.9 kW/m^2. The data points are averaged over five pixels around the middle of the channel.

The evolution of the heat flux distribution along the channel is depicted in Fig. 3. Each data point in this plot is an averaged value over five pixels arranged in a straight line normal to the flow direction around the middle of the channel. The heat flux distribution in the uncoated part of the mini-channel is characterized by a highly dynamic behavior with sharp maxima and deep minima, which can be attributed to the effect of the bubble passing through the channel. The heat flux in the transition zone adjacent to the boundary between the uncoated and coated parts is relatively homogeneous and stationary. At the upstream side the transition region is bounded by a sharp heat flux maximum. Beyond this point of maximum, which can be attributed to the heat conduction in the heating foil, the heat flux is again homogeneous and stationary, but at a much lower level in comparison to the transition region and the average heat flux at the uncoated part.

The results of the preliminary experiment show that an efficient heat transfer at the nanofiber-coated heater can be expected over a short length, which is comparable to the length of the transition region. In the following series of the experiments a spatially-periodic coating of the heater has been used. A series of images in Fig. 4 shows an elongated bubble passing through an uncoated part of the heater. After the rear part of the bubble crosses the boundary toward the uncoated part, the emergence of small bubbles at the boundary can be observed. The growth and motion of these bubbles can be followed in the last two images in Fig. 4.

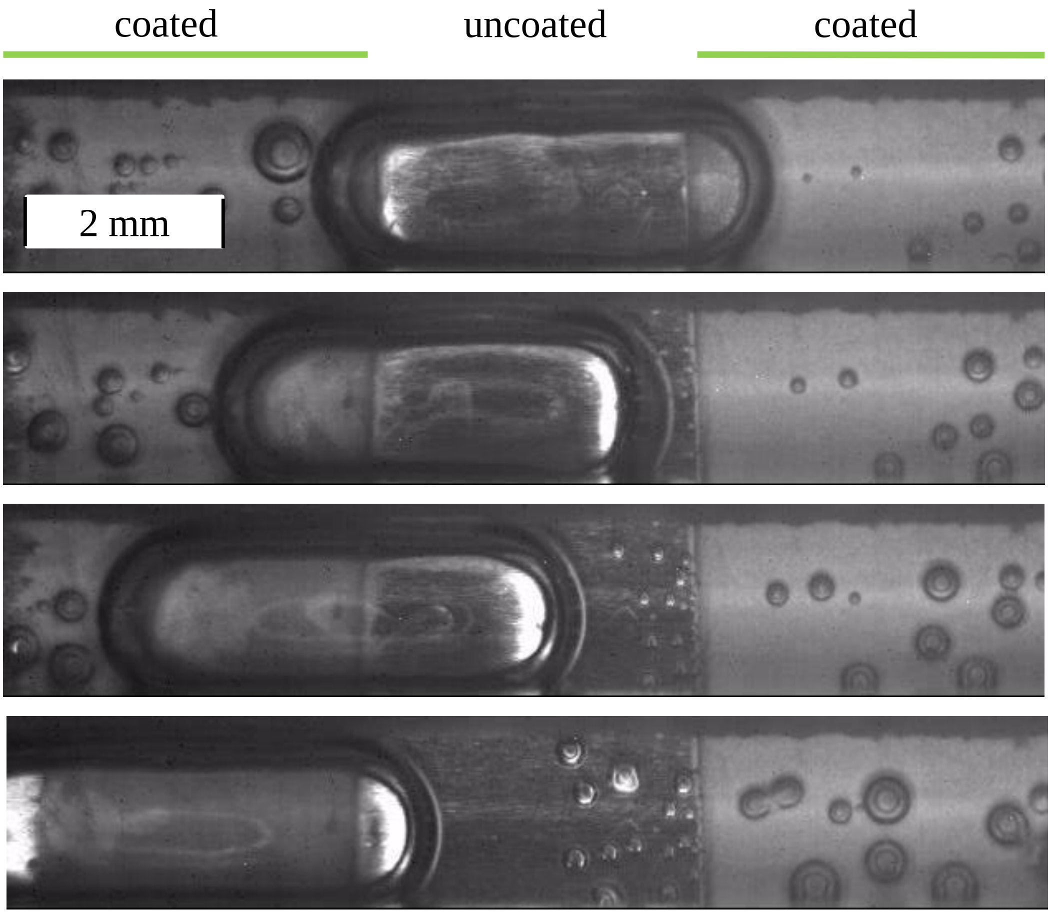

Fig. 4. Typical flow pattern sequence in a mini-channel with spatially-periodic nanofiber coating. $Re = 313$, $q_h = 24.3$ kW/m^2.

A series of images in Fig. 5 shows the video sequences of flow patterns together with the heat flux distribution (in relation to the heat flux applied to the heater). At the time moment corresponding to Fig. 5a the front of the elongated Taylor bubble reaches the edge of the coated region. The distribution of heat flux is relatively homogeneous revealing regions of higher heat flux corresponding to position of small bubbles. As the elongated bubble flows over the uncoated region of the heater, the film separating the bubble from the heater surface breaks up producing a dry spot (Fig. 5b, upper image, a white oval region near the lower edge of the field of view). This spot corresponds to the region of a very low heat flux (Fig. 5b, lower image, a dark blue oval patch near the lower edge of the field of view). The dry spot increases in size (Fig. 5c) and eventually occupies the entire uncoated portion of the heater in the field of view (Fig. 5d). It should be emphasized that the elongated bubble in the field of view covers some parts of the coated surface as well. The heat flux transferred from the coated parts of the heater to the fluid is only insignificantly reduced in comparison with the regions unaffected by the bubble. Figure 5e shows the next stage of the Taylor bubble flowing over the observation region. The rear edge of the bubble moves over the bare heater surface. A small region with high heat flux can be observed behind the bubble. This phenomenon can be attributed to the very high evaporation rate in the vicinity of the advancing contact line [21, 22]. This effect could not be observed as the rear edge of the bubble moves over the coated part of the heater (Fig. 5c). In general, during the entire cycle, the distribution of the heat flux is much more homogeneous over the coated parts of the heater in comparison with the uncoated parts.

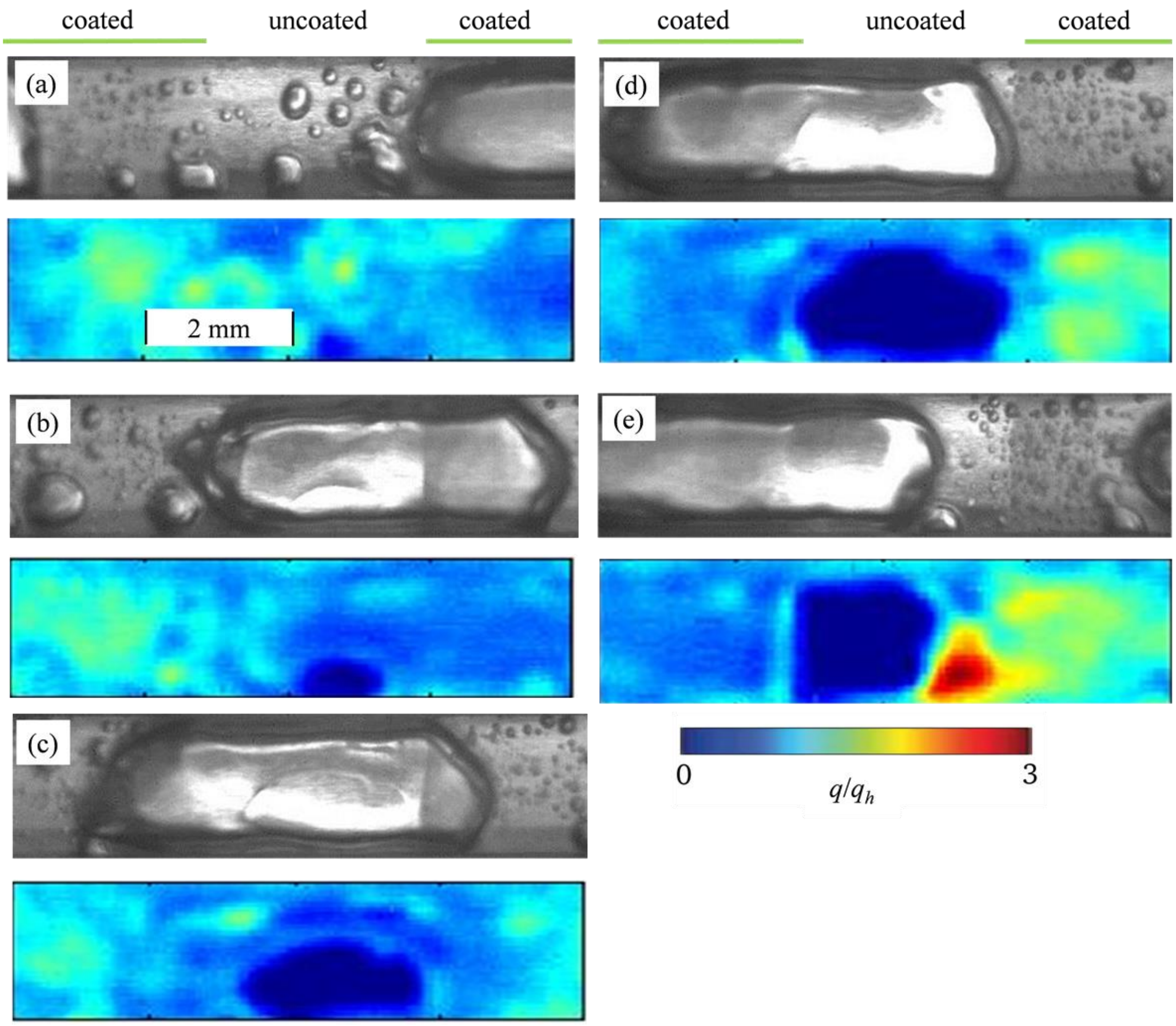

Fig. 5. Typical flow pattern sequence and relative heat flux distribution in a mini-channel with spatially-periodic nanofiber coating. Re = 300, q_h = 40 kW/m^2. The length of the field of view is 8 mm. Time moments: (a) 0 ms, (b) 17 ms, (c) 27 ms, (d) 34 ms, (e) 41 ms.

The heat transfer characteristics in flow boiling in a mini-channel with the spatially-periodic coating (approximately 3 mm-long coated parts separated from each other by 4 mm-long uncoated parts) are illustrated in Fig. 6. The heat flux transferred to the fluid, q (Fig. 6a), and the wall superheat (the difference between the wall temperature, T, and the saturation temperature, T_{sat}, Fig. 6b) are averaged over time and over five pixels in the middle of the channel. The heat transfer coefficient, h (Fig. 6c) has been determined using the standard definition $h = q/(T - T_{\text{sat}})$.

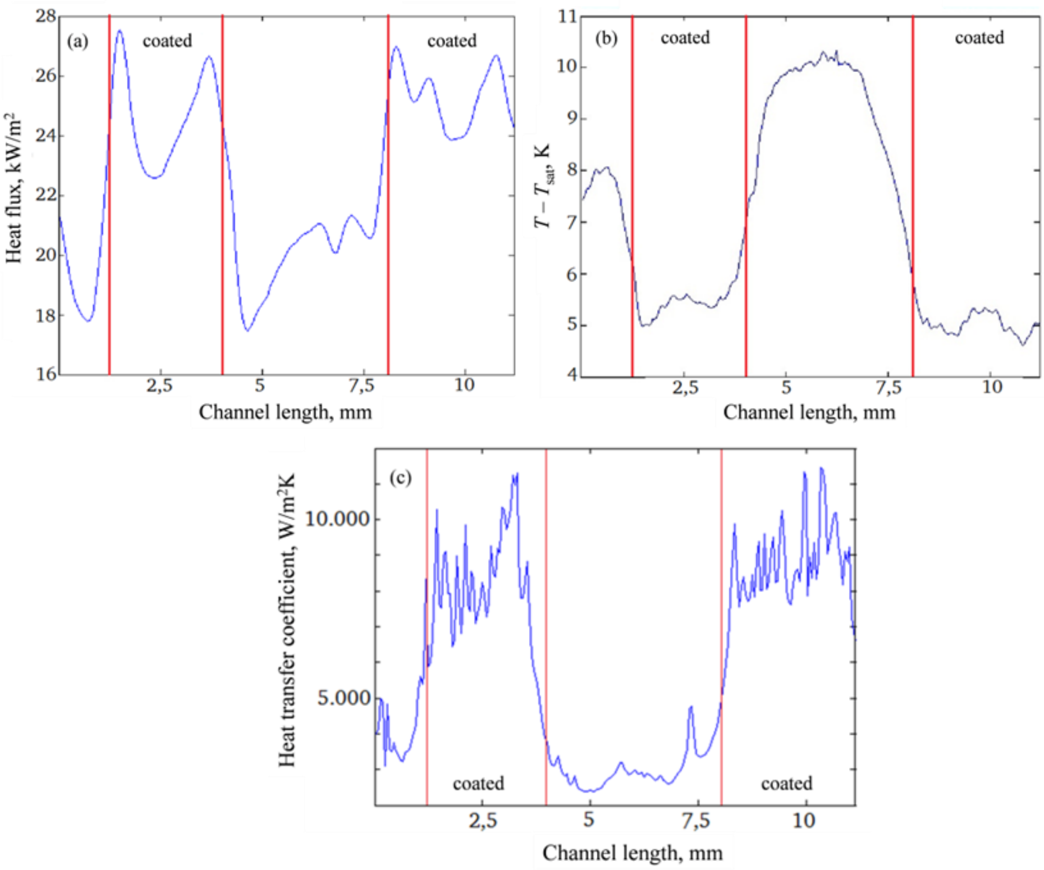

Fig. 6. Time-averaged heat flux distribution (a), wall superheat (b) and heat transfer coefficient (c). *Re* = 313, q_h = 35.5 kW/m^2. The data points are averaged over five pixels around the middle of the channel.

It is seen that significantly higher heat flux is transferred to the fluid at the areas coated with the nanofiber mat (an increase of the heat flux in about 25-30% in average). Peaks of the heat flux are observed near the boundaries between the uncoated and coated parts (Fig. 6a). The coated parts are also characterized by a 50% lower superheat compared to the uncoated ones, i.e. are much more efficiently cooled (Fig. 6b). Finally, the heat transfer coefficient is one order of magnitude higher at the coated parts in comparison to the uncoated parts of the heater (Fig. 6c). This result shows that there is a great potential in using spatially-periodic nanofiber mat coatings for heat transfer enhancement during flow boiling. Qualitatively similar results have been obtained at different flow and heating rates. For example, at the

Reynolds number of 387 and the applied wall heat flux of 36.1 kW/m^2 a significant decrease in the superheat (by 8 K) and increase in the heat flux transferred to the fluid (around 60%) has been recorded at the domains of the heater coated with nanofiber mats (Fig. 7).

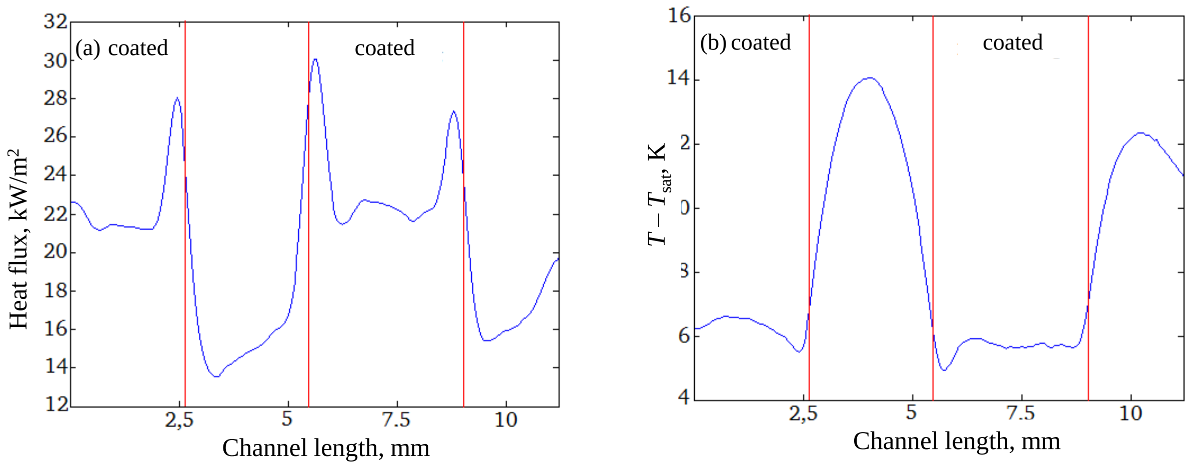

Fig. 7. Time-averaged heat flux distribution (a) and wall superheat (b). *Re* = 387, q_h = 36.1 kW/m^2. The data points are averaged over five pixels around the middle of the channel.

The temporal evolution of the heat flux transferred to the fluid, as well as of the wall superheat for heaters with a spatially-periodic coating is shown in Fig. 8 for *Re* = 313, q_h = 35.5 kW/m^2. The heat flux on the uncoated parts is characterized by sharp maxima and deep minima sustained over a long period. The temperature evolution at the uncoated part of the heater exhibits large plateaus of high superheat values. The distributions of heat flux and temperature are much more homogeneous in time on the coated parts of the heater in comparison to the uncoated ones, which is also in agreement with the results of the preliminary experiments (Fig. 3). In the following section we discuss the mechanisms of the observed phenomena.

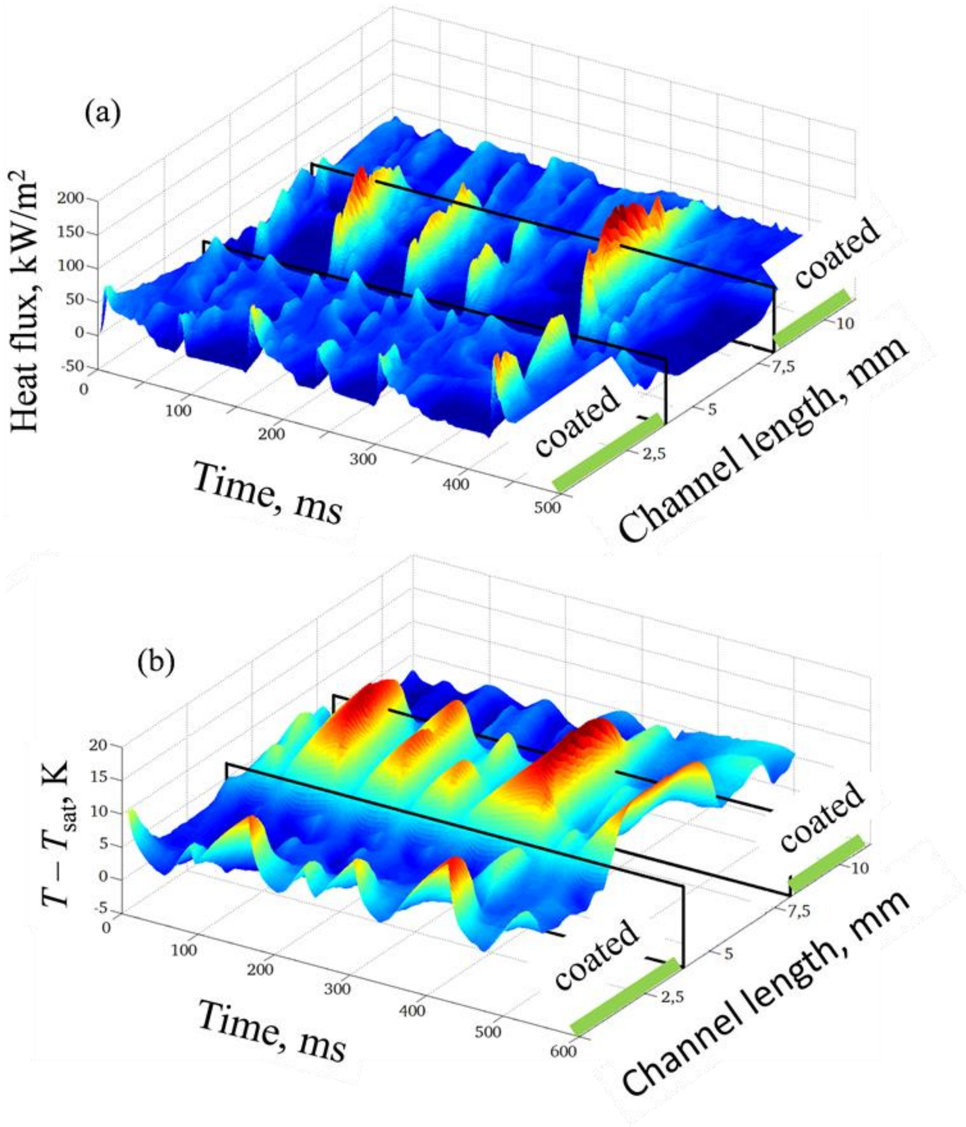

Fig. 8. Transient heat flux distribution (a) and transient wall superheat (b). *Re* = 313, q_h = 35.5 kW/m^2.

4. Discussion

The nanofiber coatings tend to retain liquid coolant and distribute it over large areas inside its fluffy porous structure [8-16, 23, 24]. As an elongated bubble flows over an uncoated part of the heater and the film under the bubble dries out, the local heat transfer rate dramatically decreases and the wall superheat significantly increases (Fig. 8b). As the bubble passes the heater portion coated with nanofiber mat, the capillary forces and viscous dissipation retain the liquid in the porous structure. Evaporation of this liquid, which is responsible for the heat transport from the heated wall, prevents the development of local and transient temperature peaks. This phenomenon leads to the homogeneous temporal and spatial distributions of heat flux and temperature over the coated regions and to a higher heat transfer coefficient there.

One can assume that coating the entire heater surface with nanofiber mat would inevitably lead to a significant heat transfer enhancement. However, it is not true. An intensive evaporation of liquid near the hot wall results in production of large amount of vapor. This vapor apparently cannot leave the porous layer in the direction normal to the mat, and therefore forms a thermally insulating layer. This leads to a decrease in the heat transfer rate and to overheating of the wall. The vapor leaves the nanofiber mat in the form of bubbles at the boundary between the coated and uncoated parts. Simultaneously the coolant liquid enters the porous structure at the same boundary. As a result, in the area adjacent to this boundary (the transition region in Fig. 2) the nanofiber mat encapsulates a two-phase vapor-liquid mixture. The evaporation of liquid from the pores in the transition zone contributes to the overall heat transfer. In contrast, the coated region far away from the boundary with the bare heater surface does not contribute to the overall heat transfer (see Fig. 2, the region of low heat flux to the right from the transition region). Therefore, instead of the entire heater area coating, the patterned periodic coating is beneficial to use in order to significantly enhance the heat transfer. The optimal size of the coated patches and the optimal distance between the patches will be determined in future parametric studies. It should be emphasized that the optimal patches pattern geometry could depend on the fluid properties, thermodynamic conditions, fluid flow rate and the applied heat flux.

Other important parameters of the nanofiber coating include the chemical composition of the fibers and the coating thickness. The advantage of relatively thick coatings is in a large amount of liquid which can be retained inside a single patch. In order to sustain a high and nearly constant heat transfer rate, this amount of liquid should be at least enough to be evaporated completely in a time which it takes for an elongated Taylor bubble to flow over the patch. The disadvantage of thick coatings is in the increase of the hydrodynamic resistance and deceleration of the fluid flow along the channel and also in the increased thermal resistance, if the coating is predominantly filled with vapor. The optimization of the coating parameters toward the maximal possible heat transfer enhancement is aimed in future.

5. Conclusions

Heat transfer during flow boiling in a mini-channel with nanofiber-coated heater surface has been studied experimentally. The temperature and heat flux distribution at the heater surface have been determined using high-speed infrared thermography.

Coating of a large area of the heater with a single nanofiber patch does not lead to heat transfer enhancement. This can be explained by formation of vapor layer within the porous coating which cannot escape into the liquid phase due to the arrangement of the nanofibers parallel to the wall.

Spatially-periodic coating of the heater leads to significant heat transfer enhancement, amounting to an order of magnitude increase of the heat transfer coefficient over the coated domains compared to the uncoated domains. This can be attributed to the fact that the liquid is retained in the porous layer due to capillary forces as a Taylor bubble flows over the heater, whereas local dry-out is observed as the bubble passes over the uncoated heater domains. An additional potential source of the heat transfer enhancement is the release of small vapor bubbles at the boundaries between the coated and uncoated domains.

Acknowledgements

A.L.Y., S.S.-R. and R.P.S. were supported by NASA (Grant No. NNX13AQ77G). T.G.-R. acknowledges the financial support of EC through the Marie Curie Initial Training Network "Complex Wetting Phenomena" (CoWet), Grant Agreement no. 607861.

References

[1] A. Bar-Cohen, C. A. Holloway, Thermal science and engineering – from macro to nano in 200 years, IHTC15-FL01 Proc. 15th International Heat Transfer Conference, August 10-15, 2014, Kyoto, Japan.

[2] A. M. Jacobi, J. R. Thome, Heat transfer model for evaporation of elongated bubble flows in microchannels, J. Heat Transfer, 124 (2002) 1131-1136.

[3] J. R. Thome, V. Dupont, A. M. Jacobi, Heat transfer model for evaporation in microchannels. Part I: presentation of the model. Int. J. Heat Mass Transfer**,** 47 (2004) 3375-3385.

[4] N. Schweizer, M. Freystein, P. Stephan, High resolution measurement of wall temperature distribution during forced convective boiling in a single minichannel, FEDSM-ICNMM2010-30273, Proc. ASME 2010 3rd Joint US-European Fluid Engineering Summer Meeting and 8th International Conference on Nanochannels, Microchannels and Minichannels FEDSM-ICNMM2013, August 1-5, 2010, Montreal, Canada.

[5] Z. Yao, Y. W. Lu, S. G. Kandlikar, Micro/nano hierarchcal structure in microchannel heat sink for boiling enhancement, Proc. IEEE 25th International Conference on Micro Electro Mechanical Systems (MEMS), January 29 – February 2, 2012, Paris, France.

[6] D. Li, G. S. Wu, W. Wang, Y. D. Wang, D. Liu, D. C. Zhang, Y. F. Chen, G. P. Peterson, Enhancing flow boiling heat transfer in microchannels for thermal management with monolithically-integrated silicon nanowires. Nano Letters, 12 (2012) 3385-3390.

[7] S. Bhavnani, V. Narayanan, W. Qu, M. Jensen, S. Kandlikar, J. Kim, J. Thome, Boiling augmentation with micro/nanostructured surfaces: Current status and research outlook. Nanoscale and Microscale Thermophysical Engineering, 18 (2014) 197-222.

[8] R. Srikar, T. Gambaryan-Roisman, C. Steffes, P. Stephan, C. Tropea, A. Yarin, Nanofiber coating of surfaces for intensification of spray or drop impact cooling. Int. J. Heat Mass Transfer, 52 (2009) 5814-5826.

[9] A. N. Lembach, H. B. Tan, I. V. Roisman, T. Gambaryan-Roisman, Y. Zhang, C. Tropea, A. L. Yarin, Drop impact, spreading, splashing and penetration into electrospun nanofiber mats. Langmuir, 26 (2009) 9516-9523.

[10] S. Sinha-Ray, Y. Zhang, A. L. Yarin, Thorny devil nanotextured fibers: the way to cooling rates on the order of 1 kW/cm^2. Langmuir, 27 (2011) 215-226.

[11] C. M. Weickgenannt, Y. Zhang, A. N. Lembach, I. V. Roisman, T. Gambaryan-Roisman, A. L. Yarin, C. Tropea, Non-isothermal drop impact and evaporation on polymer nanofiber mats. Phys. Rev. E, 83 (2010) 036305.

[12] C. M. Weickgenannt, Y. Zhang, S. Sinha-Ray, I. V. Roisman, T. Gambaryan-Roisman, C. Tropea, A. L. Yarin, The inverse-Leidenfrost phenomenon on nanofiber mats on hot surfaces. Phys. Rev. E**,** 84 (2011) 036310.

[13] S. Sinha-Ray, A. L. Yarin, Drop impact cooling enhancement on nano-textured surfaces. Part I: Theory and results of the ground (1 g) experiments. Int. J. Heat Mass Transfer, 70 (2014) 1095-1106.

[14] S. Sinha-Ray, S. Sinha-Ray, A. L. Yarin, C. M. Weickgenannt, J. Emmert, C. Tropea, Drop impact cooling enhancement on nano-textured surfaces. Part II: Results of the parabolic flight experiments [zero gravity (0g) and supergryvity (1.8g)]. Int. J. Heat Mass Transfer, 70 (2014) 1107-1114.

[15] S. Jun, S. Sinha-Ray, A. L. Yarin, Pool boiling on nano-textured surfaces. Int. J. Heat Mass Transfer, 62 (2013) 99-111.

[16] R. P. Sahu, S. Sinha-Ray, S. Sinha-Ray, A. L. Yarin, Pool boiling on nano-textured surfaces comprised of electrically-assisted supersonically solution-blown, copper-plated nanofibers: Experiments and theory. Int. J. Heat Mass Transfer, 87 (2015) 521-535.

[17] D. H. Reneker, A. L. Yarin, E. Zussman, H. Xu, Electrospinning of nanofibers from polymer solutions and melts. Advances in applied mechanics, 41 (2007) 43-346.

[18] D. H. Reneker, A. L. Yarin, Electrospinning jets and polymer nanofibers. Polymer 49 (2008) 2387-2425.

[19] A. L. Yarin, B. Pourdeyhimi, S. Ramakrishna, Fundamentals and Applications of Micro- and Nanofibers (Cambridge University Press, Cambridge, 2014).

[20] M. Freystein, C. Kirse, P. Stephan, Bubble coalescence and moving contact line evaporation during flow boiling in a single minichannel, ICNMM2013-73043, Proc. ASME 2013 11th International Conference on Nanochannels, Microchannels and Minichannels ICNMM2013, June 16-19, 2013, Sapporo, Japan.

[21] P. Stephan, C. Busse, Analysis of the heat transfer coefficient of grooved heat pipe evaporator walls. Int. J. Heat Mass Transfer, 35 (1992) 383-391.

[22] C. Kunkelmann, K. Ibrahem, N. Schweizer, S. Herbert, P. Stephan, T. Gambaryan-Roisman, The effect of three-phase contact line speed on local evaporative heat transfer: Experimental and numerical investigations. Int. J. Heat Mass Transfer, 55 (2012) 1896-1904.

[23] R. P. Sahu, S. Sinha-Ray, A. L. Yarin, B. Pourdeyhimi, Drop impacts on electrospun nanofiber membranes. Soft Matter, 8 (2012) 3957-3970.

[24] T. Gambaryan-Roisman, Liquids on porous layers: Wetting, imbibition and transport processes. Current Opinion in Colloid and Interface Science, 19 (2014) 320-335.